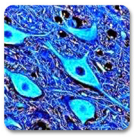

Journal of Histology & Histopathology
ISSN 2055-091X | Volume 4 | Article 13

HOAJ
Herbert Open Access Journals

Special Section | Morphological bases of human diseases | Original Research Open Access

The effects of different inhibitory pathways of prostaglandin E_2 biosynthesis on renomedullary interstitial cells in rats: a multidisciplinary study

Sibel Demirci Delipinar[1*], Huseyin Sonmez[2], Hakan Ekmekci[2], Leyla Ayse Erozenci[3] and Ismail Seckin[1]

*Correspondence: sibell.demirci@gmail.com

[1]Department of Histology and Embryology, Cerrahpasa Medical Faculty, Istanbul University, Istanbul, Turkey.
[2]Department of Biochemistry, Cerrahpasa Medical Faculty, Istanbul University, Istanbul, Turkey.
[3]Department of Medical Oncology, Vrije Universiteit, Holland.

Abstract

Renomedullary interstitial cells (RMICs) are the most dominant cell type in inner renal medulla. Their most distinct characteristic is the presence of multiple lipid droplets in their cytoplasm. These lipid droplets are believed to be the storage units for precursors of prostaglandins (PGs), prostacyclin and medullipin. Especially prostaglandin E_2 (PGE_2) is synthesized by RMICs in kidney. PGs are produced by three key steps: 1) Arachidonic acid (AA) release from membrane phospholipids by the action of phospholipase A_2 (PLA_2); 2) Formation of prostaglandin H_2 (PGH_2) from AA by the action of cyclooxygenases (COXs); 3) Specific PG synthesis metabolism from PGH_2. PG biosynthesis can be regulated via activation or inhibition of these steps. In this study, we examined the effects of PGE_2 inhibition in different steps on RMIC function, the number of lipid droplets, medullary hyaluronan (HA) content and cell viability. We formed four groups (n=8): First group was control and treated with intraperitoneal (ip) 0.9% saline. Second group in which we inhibited AA release from membrane phospholipids was injected with ip dexamethasone (DEX) (2 mg/kg, 10 days); third group was treated with ip indomethasine (IND) (1 mg/kg, 10 days) to inhibit non-specific COX at the stage of PGH_2 formation from AA; and the fourth group was injected with ip celecoxib (CXB) (1 mg/kg, 10 days) to examine selective cyclooxygenase-2 (COX-2) inhibition.

We dissected renal medulla of the sacrificed animals after 10 days to analyze with light and electron microscopy. We counted the lipid droplets in 50 random RIMCs for each animal (x6.000 magnification) in electron microscopy. Our morphometric analysis showed that the number of lipid droplets was significantly decreased in DEX group and was significantly increased in IND and CXB groups when compared to control. In addition, medullary HA content and CD44 immunoreactivity were significantly increased in all groups when compared to control. When we analyzed cell viability, we found that RMIC apoptosis was significantly higher in PGE_2 inhibited groups when compared to control. Besides this, 24-hour urine values collected on the 10th day were significantly increased in dexamethasone and indomethacin groups; but in celecoxib group the values were similar to control. These results indicate that lipid granules may be numerical and functionally influenced from PGE_2 changes, these granules may be storage units of AA, functional changes in RMICs by PGE_2 may influence HA quantity of medullary interstitium and urine volume, and finally PGE_2 inhibition may lead to RMIC apoptosis.

Keywords: Kidney, Non steroidal anti-inflammatory drugs, Prostaglandin E_2, Renomedullary interstitial cells, Cyclooxygenase-2

Introduction

The kidney has both pro- and anti-hypertensive activities [1,2]. Renomedullary interstitial cells (RMICs) are the most abundant cell type in the inner renal medulla and they have several char-

doi: 10.7243/2055-091X-4-13

acteristic features. Their most distinctive characteristic is the presence of multiple lipid droplets in their cytoplasm. The investigators suggest that RMICs are secretory cells because of their well-developed rough endoplasmic reticulum (RER), Golgi complex and the content of multiple lipid droplets [3]. Therefore, they are referred to as the lipid-containing type 1 interstitial cells, which are the principal cells in the inner medulla [4]. In 1969, Bohman and Maunsbach isolated lipid droplets from RMICs and found that they had a vasodepressor activity. The content of these lipid granules are believed to be storage units for precursors of prostaglandins (PGs), prostacyclin and medullipin [1]. The amount and the size of lipid droplets are shown to be involved in the changes of diuretic stages, water-salt balance, renal perfusion pressure (RPP) and medullary blood flow (MBF) [1]. RMICs are often arranged in rows between the loops of Henle and vasa recta, with their long axes being perpendicular to those of adjacent tubules and vessels, thus resembling the rungs of a ladder [3]. This anatomic arrangement suggests that RMICs may play an important role in maintaining urinary concentrating ability via preventing the axial diffusion in concentration gradient [5,6]. Studies demonstrate that the transplants of fragments from the renal medulla or of the cultured RMICs reverse renoprival hypertension [1,7-13]. The biochemical analyses of these medullary transplants show the presence of prostaglandins (PGs), triglycerides, cholesterol esters and free fatty acids [14]. At the end of these studies, three types of substances with potential antihypertensive properties are derived from the kidney medulla [12]:

1) Prostaglandins (PGs)
2) Antihypertensive neutral renomedullary lipid (ANRL)
3) Antihypertensive polar renomedullary lipid (APRL).

Cell culture studies demonstrate that PGs, especially prostaglandin E_2 (PGE_2) are synthesized by RMICs in the kidney [3,7,12,13]. PGs are produced by three key steps: 1) Arachidonic acid (AA) release from membrane phospholipids by the action of phospholipase A_2 (PLA_2); 2) Formation of prostaglandin H_2 (PGH_2) from AA by the action of cyclooxygenases (COXs); 3) Specific PG synthesis metabolism from PGH_2. PG biosynthesis can be regulated via activation or inhibition of these steps. Various researchers work with PGE_2 stimulators and inhibitors in their renal medulla studies; however, we are unable to find a research on inhibition before AA release in the literature. We believe that using pre-AA release inhibitors in addition to COX inhibitors better clarify the characteristic of lipid droplets and whether their activity in PGE_2 synthesis continues via other pathways or not. Selective cyclooxygenase-2 (COX-2) inhibitors (coxibs) and several non-selective COX-inhibiting nonsteroidal anti-inflammatory drugs (NSAIDs) block endogen PG synthesis. However, studies suggest that, this inhibition leads to RMIC apoptosis [15-20]. Furthermore, hyaluronan (HA) which is a negatively charged glycosaminoglycan (GAG) found in renal interstitium and in the synthesis by RMICs, may play an important role in maintaining of water homeostasis [21,22]. The high concentrations of HA in the kidney medulla support tubules and blood vessels and it is important for urine concentration [22]. HA also has a wondrous renal water handling capacity which is important for maintaining the concentration gradient and affects water transport in renal medulla [21-23].

In this study, we examine the effect of inhibition of PGE_2 synthesis in different pathways on RMIC function, the number of lipid droplets, medullary HA content and cell viability. The glucocorticoids inhibit PLA_2 enzyme in AA release stage from membrane phospholipids. Thus, they reduce the formation of all the eicosanoids (PGs, prostacyclins, thromboxanes and leukotrienes). For this reason, we inhibit AA release with PLA_2 inhibition by using dexamethasone (DEX) which is a glucocorticoid. AA released via PLA_2 is converted into PGG_2 by being presented to COX (prostaglandin H synthase, PGHS). Then, COXs generate intermediate endoperoxide PGG_2 which is a substrate for terminal synthases by reducing PGG_2. We inhibit PGE_2 formation from PGH_2 in two different pathways via COX. For this study, we use indomethacin (IND) which is a non-selective COX inhibitor (COX-1 and COX-2 inhibition), and celecoxib (CXB) which is a selective COX-2 inhibitor.

We aim to analyze the morphological changes and the number of lipid droplets of RMICs in different PGE_2 inhibition groups. Furthermore, we investigate how medullary HA content, amount of urine and cellular viability from PGE_2 inhibition are affected. Finally, we search for an answer: Are the lipid droplets the storage units for PG precursor AA?

Methods

Thirty-two adult male Wistar albino rats weighing 180-200g (Experimental Animals Reproduction and Research Laboratory, Istanbul University Cerrahpasa Medical Faculty, Turkey) were housed in individual cages in a temperature- and humidity- controlled room with a 12-h light/dark cycle. They were fed with standard rat chow and had free access to tap water. Rats were divided into four groups (n=8). Control group was daily injected with 1 ml ip 0.9% NaCl solution during 10 days. Second group was daily injected with ip 2 mg/kg dexamethasone during 10 days. Third group was injected with ip 1 mg/kg indomethasine during 10 days and the last group was injected with ip 1 mg/kg celecoxib during 10 days. All rats were sacrificed under anesthesia at the end of the study (10th day) according to the regulation of animal ethical committee of Istanbul University.

Biochemical analyses

24 h urine samples were collected on the 1st and 10th days from animals. Urine volumes were measured using micropipets and pH values were measured using pH-indicator strips (Merck; pH:0-14). The blood samples were collected on the 10th day from animals via intracardiac-punction method. Samples were taken in heparinisetubes and centrifuged in 1500 rpm for 15 minutes. Serum samples collected and PGE_2

doi: 10.7243/2055-091X-4-13

levels were determined by ELISA method.

Light microscopical analyses
Renal medullar tissues were fixed in 10% neutral buffered formalin dehydrated with graded ethanol and embedded into paraffin. The sections of 5µm thickness were placed onto poly-*l*-lysine-coated slides. Histological determination of renal medullar HA content was carried out by Alcian blue staining (pH: 2.5). The evaluation of the Alcian blue staining was done utilizing H-SCORE from renal papilla and inner medulla, using randomly selected 5 different fields for each slide, x40 magnification.

Immunohistochemical analyses
The sections of 5 µm thickness were placed onto poly-*l*-lysine-coated slides. After deparaffinization and rehydration samples were placed in citrate buffer (pH6), antigen retrieval was performed by treating the samples in a microwave oven at 750 W for 5 min three times, and then slides were washed in PBS. Immunohistochemistry procedure was performed using standard streptavidin-biotin-peroxidase method. Endogenous peroxidase activity was blocked by 3% hydrogen peroxide (Dako, Glostrup, Denmark). Each section was then incubated for 15 minutes at room temperature with blocking solution to block cellular peroxidase activity. After blocking, sections were incubated with primary antibodies mouse anti-rat CD44 diluted 1:100 (Life Span Biosciences, USA) and rabbit anti-human, rat, mouse active caspase-3 diluted 1:100 (Millipore) for 1 hour at room temperature, then washed with PBS. Specific staining was performed with biotinlated universal secondary antibody and horse radish peroxidase streptavidin-complex. Immunoreactivity was developed using amino-ethyl-carbazole as chromogen (Invitrogen). The sections were counter-stained with Mayer's hematoxylin and mounted with glycerol gelatin (Sigma). All incubations were performed in a moist chamber at room temperature. As for negative control, distilled water was performed instead of primary antibody.

Electron microscopical analyses
After necropsy, the left kidney medulla was immediately divided into 1mm^3 pieces for transmission electron microscopy. They were firstly fixed in 3% glutaraldehyde in a 0.1 M phosphate buffer solution (PBS), post-fixed by 1% OsO_4 prepared in the same buffer solution, dehydrated and embedded into araldite medium. Semi-thin sections were cut into 1 µm thickness by glass knives to help of the ultra microtome and stained with 1% toluidine blue (prepared with 1% borax in bidistilled water). The sections were examined under a binocular light microscope using immersion objective. Ultra-thin sections were obtained in 50 nm thickness onto copper grids (200 meshes) with the same microtome, stained with uranyl acetate and lead citrate and they were investigated by transmission electron microscope (Jeol JEM 1011).

Morphometric studies
We obtained ultra-thin sections from one animal in each experimental group and counted lipid droplets in randomly chosen 50 different RMICs with EM micrographs (x6000 magnification). Data was statistically evaluated.

H-Score and semi-quantitative evaluations
The evaluations of the alcian blue staining and immunohistochemical staining were done utilizing H-SCORE. From each randomly selected slides per animal, five different fields were evaluated. Stainings were scored in a semi-quantitative fashion that included the intensity of specific staining in sections. The evaluations were recorded as values between 0-300 of five intensity categories: 0 (none), 0-75 (weak but detectable above control), 75-150 (distinct), 150-225 (dense), 225-300 (intense). Two observers blinded to the experimental groups performed the H-SCORE. For each tissue, obtained an average H-SCORE value. (0:negative; 1:weak positive; 2:positive; 3:dense positive; 4:very dense positive and presented in **Figure 1** and **Table 1**).

Statistical analyses
Statistical analyses of 1st and 10th days urine volumes, 1st and 10th days urine pH values, PGE_2 values in blood serum, HSCORE values of alcian blue staining and immunohistochemistry analyses and the number of lipid droplets were compared by One-Way ANOVA tests. Statistical calculations were performed using Sigma Stat for Windows, version 3.0 (Jandel Scientific, San Rafael, CA). Comparisons were made versus the inhibition groups as a control. Probability values of less than 0.05 ($p<0.05$) were considered significant; values are presented as mean ±SEM.

Results
Biochemical findings
In control and experimental groups, urine volumes (ml/24 hours) and pH (0-14) values are shown in **Table 1** and **Figure 1**. 1st day urine volumes were not significantly different from each other ($p>0.05$). 10th day urine volumes were significantly different between control and experiment groups ($p=<0.001$). Urine volumes were found to increase in DEX and IND groups, while they were similar in CXB groups when compared with control (**Table 1** and **Figure 1**). The pH values of 1st and 10th day urine samples were not statistically significant ($p>0.05$) (**Table 1** and **Figure 1**). We validated our experiment by measuring PGE_2 levels by ELISA, in blood serum taken on the 10th day. In all inhibitions groups, PGE_2 levels were shown to be significantly lower than control ($p=<0.05$) (**Table 1** and **Figure 1**).

Light microscopic findings
Alcian blue dyes non-sulphatated acid mucopolysaccharides and acetic mucins. In this study, we used this dye to determine HA, a non-sulphatated GAG in interstitial field [**24**]. HA levels were shown to be significantly elevated in both areas in inhibition groups when compared to control ($p<0.05$) (**Table 1**)

doi: 10.7243/2055-091X-4-13

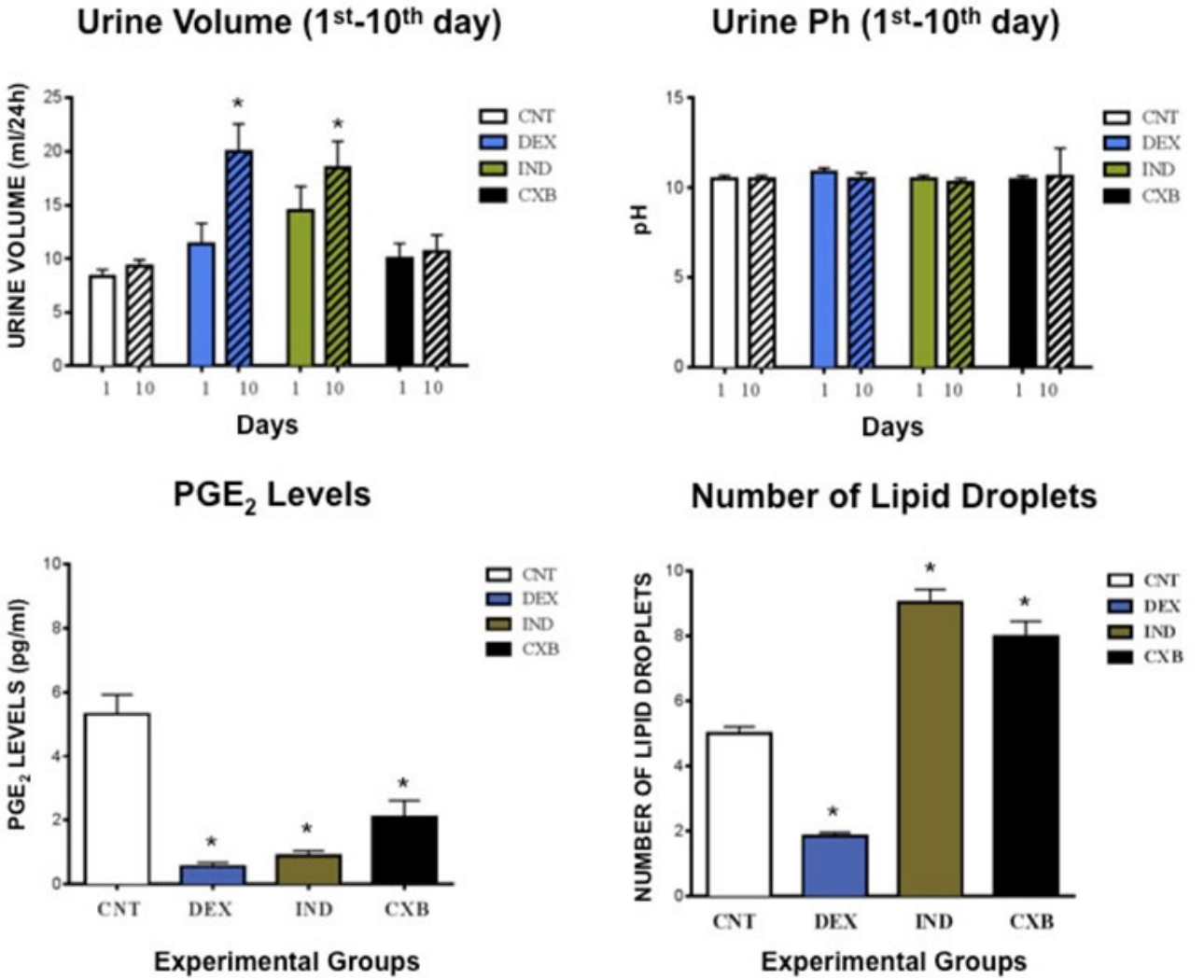

Figure 1. The graphics of urine volume, urine pH, serum PGE_2 levels and number of lipid droplets. The groups being statistically different from control group remarqued wıth star.

Table 1. All data were given in the table.

GROUPS	1st day urine volume (ml/24h)	10th day urine volume (ml/24h)	1st day urine pH (0-14)	10th day urine pH (0-14)	PGE_2 levels (pg/ml)	H-SCORE Values of Alcian Blue Staining		H-SCORE values of Cas-3 and CD44 immun-positivity		Number Of Lipid Droplets
						Papilla	Inner Medulla	Cas-3	CD44	
CNT	8,85	9,65	10,5	10,5	5,285	2	2	2	2	4,9925
DEX	13,2	21	11	10,5	0,406	3	3	3	3	1,85
IND	13,45	17,15	10,5	10	1,115	4	4	3	4	9,02
CXB	9,3	8,8	10,5	10	1,690	4	4	3	3	7,9625

doi: 10.7243/2055-091X-4-13

(**Figure 1** and **2**). Semi-thin sections were dyed with toluidine blue and examined with immersion objective (x100). Increased lipid droplets were observed in groups where PGE_2 cannot be produced because of the COX inhibition after AA step (IND, CXB) (**Figure 2**).

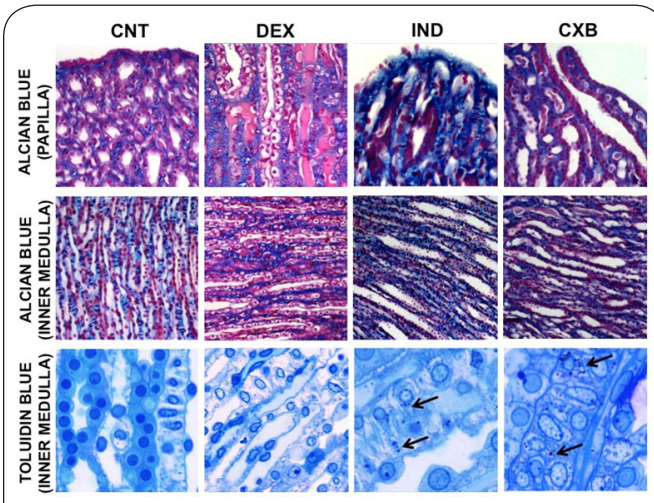

Figure 2. The Alcian blue staining in renal papilla and inner medulla (Magnification: x40). The semi-thin sections dyed with toluidin blue (Magnification: x100). Arrows indicated the increase lipid droplets in COX inhibited groups (IND and DEX).

Immunohistochemical findings

Cells that show a red reaction were accepted as immune positive (**Figure 3**). In Cas-3 staining there was significant difference between groups ($p<0.05$) (**Table 1** and **Figure 1**). PGE_2 inhibition was shown to increase apoptosis when compared to control ($p<0.001$) (**Figure 3**). H-SCORE values determined for CD44 were significantly different between inhibition and control groups ($p<0.05$) (**Table 1** and **Figure 1**). PGE_2 inhibition was shown to increase CD44 receptor numbers when compared to control ($p<0.001$) (**Figure 3**).

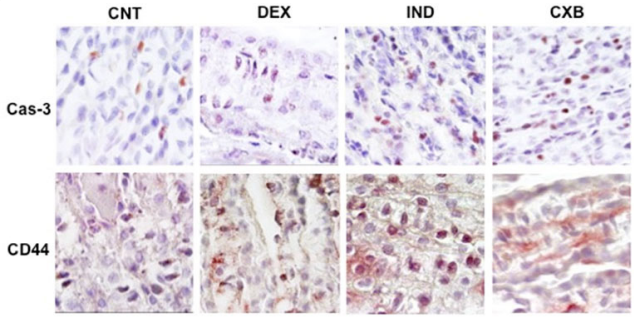

Figure 3. Immunohistochemical determination of Caspase-3 and CD44 in all groups (Magnification x100). Cas-3 and CD44 immunreactivity are shown to be increased in all inhibition groups while compared with control ($p<0.001$).

Ultrastructural findings

In control group, RMICs were found to be located between ascending and descending loops of Henle, capillaries and collecting tubules in longitudinal sections (**Figure 4**). RMICs were shown to have a poligonal shape in this group, with multiple cytoplasmic inclusions (**Figure 4**). Cytoplasmic density was normal. Most interestingly, osmophylic lipid granules of various sizes were present in the cytoplasm (**Figure 4**). Nucleus was usually round or eliptoic, with condensed heterochromatine peripherally (**Figure 4**). In some of the analyzed cells,

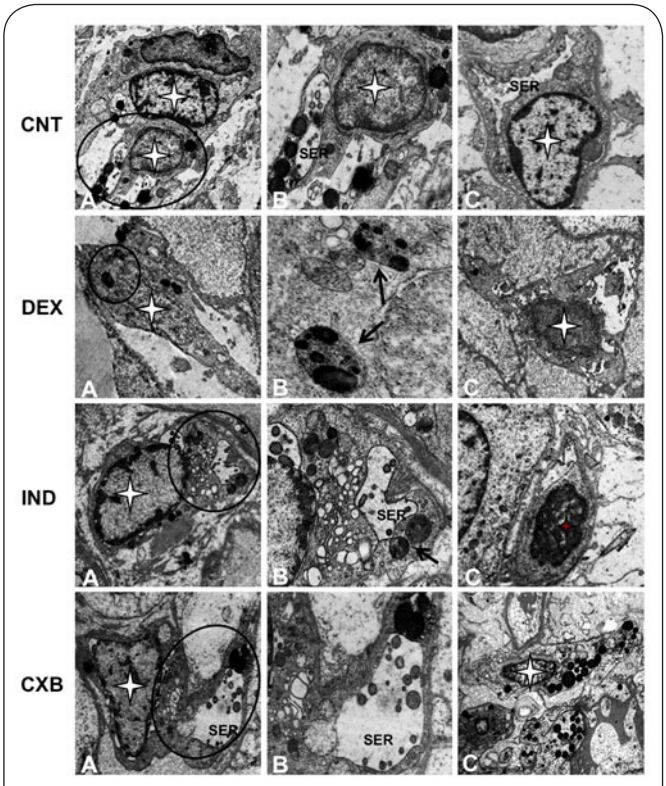

Figure 4. Electronmicrographs of RMICs in all groups. CNT: **A**) The longitudinal sections of RMICs between ascending and descending loops of Henle, capillaries and collecting tubules (x6.000). **B**) Circled area in A. SER has a normal appearance (x15.000). **C**) A RMIC in control group with normal appearance(x12.000). DEX: **A**) A RMIC with decreased lipid droplets (x6.000). **B**) Circled area in A. Lysosomes filled with granular material (arrows) (x25.000). **C**) RMICs were deprived of organelles. Empty SER cisternae and degeneration of SER membrane(x12.000). IND: **A**) Note the increased number of lipiddroplets in RMIC cytoplasm (x6.000). **B**) Circled area in **A**. Note the enlarged SER and PNCs. Arrow shows lipiddroplets in the process of degeneration to form myel instructures (x20.000). **C**) An apoptotic RMIC (x6.000). CXB: **A**) A RMIC from CXB group (x6.000). **B**) Circled area in A. Mitochondria showhy pertrophy. Note the close relation of mitochondria with enlarged SER cisternae (x20.000). **C**) Note the increased number of lipid droplets and organelles in RMICs (x6.000). Red arrow shows an apoptotic RMIC. SER: Smooth end oplasmicreticulum. White stars:RMICs. Red stars: Apoptotic RMICs.

doi: 10.7243/2055-091X-4-13

outer nuclear membrane was observed to enlarge and form perinuclear cisternas (PNC) (**Figure 4**). Round shaped mitochondria with less crista and very dense matrix were observed (**Figure 4**). Lysosomes were consisting of lysosomal material (**Figure 4**). SER and perinuclear location of Golgi complex was well determined in cells (**Figure 4**). In some of the samples, RER was also present. Free ribosomes were also observed in some samples (**Figure 4**).

In DEX group, cellular lipid droplets in RMICs were significantly decreased (**Figure 4**). Heterochromatin was increased and cells were deprived of organelles (**Figure 4**). ER cisternas were usually empty (**Figure 4**). Most specific property of these groups was endothelial hyperthrophy (**Figure 4**). Lysosomes were filled with granular material (**Figure 4**). Mitochondrion was rarely observed (**Figure 4**).

In IND group, lipid droplets in RMICs were significantly increased (**Figure 4**). Heterochromatin was increased and heterogenly located in the nucleus (**Figure 4**). ER cisternas were enlarged, containing granular material (**Figure 4**). PNCs were also enlarged with granular material (**Figure 4**). Lipid droplets stacked in cytosol, since they were not used, were marked to be degraded, engulfed in lysosomes, and then formed myelin structures (**Figure 4**). In this group, the frequency of apoptotic cells were highly increased (**Figure 4**).

In CXB group, lipid droplets in RMICs were significantly increased (**Figure 4**). Cells were euchromatic and rich in organelle, like an active cell (**Figure 4**). ER was well developed and enlarged ER cisternas were present (**Figure 4**). Also developed Golgi system had a perinuclear location. Mitochondria were observed to be hypertrophic (**Figure 4**). As in the previous group, this group also had increased apoptotic cells (**Figure 4**).

Morphometric findings

The number of lipid droplets in randomly selected 50 RMICs was counted in ultra-thin sections prepared for electron microscopy analysis, x6000 magnification. Data was analysed by One Way ANOVA (**Table 1**) (**Figure 1**). In the DEX group, where AA formation via PLA_2 was inhibited, number of lipid droplets was significantly decreased when compared with control ($p=<0.001$) (**Table 1** and **Figure 1**). Contrarily, number of lipid droplets were shown to be significantly increased in IND and CXB groups, compared to control ($p=<0.001$) (**Figure 1**).

Discussion

Kidneys are known to show pro- and anti-hypertensive activity. The pro-hypertensive effect of kidney is regulated by locally active vasopressor systems, including renin-angiotensin system; while the anti-hypertensive effect is thought to depend on vasodepressor agents [**1**,**13**].

Muirhead et al. showed that renal cortical fragment transplantation does not inhibit malign hypertension development, while transplantation of renal medullar fragments of RMICs in culture overcomes renoprival hypertension [**7**,**9-13**,**25**]. Biochemical analyses revealed that these transplants contain abundantly PGs, triglycerides, cholesterol esters and free fatty acids [**14**].

Renal medulla is the primary synthesis location for PG synthesis. Tissue culture studies on RMICs revealed that these cells are specialized in PG synthesis [**1**,**13**]. It is well known that the most specific property of RMICs is the numerous lipid droplets they contain [**1**,**3**,**8**]. The number and size of these lipid droplets change according to the species and physiological state [**1**]. The number and size of lipid droplets are reported to decrease in the 24 hours following dehydration [**1**]. In the water-restored rats, the number and size of lipid droplets increased [**1**]. Although there is not a clear connection identified between lipid droplets and diuretic state of the animals, further studies should be performed to confirm this. The content of these lipid droplets is also not completely known but they are thought to store pivotal products of PGs [**1**]. The relation between RMIC lipid droplets and renal medullar antihypertensive effect depends on these findings.

Our study also stems from the hypothesis that lipid droplets could be storage units for AA; and we examined the effect of PGE_2 inhibition at different steps on cellular lipid droplets. It is known that PGs are produced in 3 steps via renal COXs (COX-1 and COX-2) by releasing AA from membrane phospholipids [**26**]:

1. AA release from membrane phospholipids by PLA_2.
2. Production of PGH_2 from AA by COX.
3. Specific PG synthesis metabolism.

PG production can be regulated via activation and inhibition of these steps. Various researchers used PGE_2 inhibitors and stimulators in their studies on RMICs; however, we could not find any inhibition performed pre-AA-release in our literature studies. We designed this study to clarify how this kind of inhibition together with COX inhibition, and the co-use of specific and non-specific COX inhibitors in experimental groups effect lipid droplets, and whether the activity of these cells during PGE_2 production process continues using other pathways or not. In our study, we used a glucocorticoid DEX, to inhibit PG synthesis in AA release step by PLA_2; a non-specific COX inhibitor IND (NSAID), to inhibit production of PGH_2 from AA step; and a specific COX-2 inhibitor CXB (coxib).

In DEX group, cellular lipid droplet numbers were significantly decreased when compared to control. Nucleus was rich in heterochromatin and the cells were deprived of organelles, as in inactive cells. Enlarged ER cisternas were mostly empty. We assume that these cisternas are empty because PGE_2 cannot be produced, since AA synthesis is inhibited. We also observed endothelial hypertrophy and capillary narrowing in this group.

In IND group, the number of cellular lipid droplets was significantly increased. We believe this increase is the result of non-processed (because of the lack of COX) and build-up AA in the cell. Heterochromatin was found to be increased and the cellular structure was diminished and degenerated. In addition, the cells had highly enlarged ER cisternas and

doi: 10.7243/2055-091X-4-13

disturbed mitochondria and Golgi. We also observed defected lipid droplets and accumulation of these granules in lysosomes.

The number of lipid droplets showed a smaller increase in CXB group (specific COX-2 inhibition group) when compared to IND group, and that the cells in the CXB group have a richer organelle appearance suggests that PG synthesis continues, although minimally, via COX-1 pathway. The fact that PGE_2 levels measured in blood serum are higher in CXB group compared to IND supports this hypothesis. 10th day urine volumes, showing an increase in DEX and IND groups while CXB values were similar to control, also propose that COX-1 pathway has a role in PGE_2 synthesis in the CXB group. In all three groups where we inhibited PGE_2, the significant decrease in granule numbers of RMICs in pre-AA-release inhibited group by DEX, and the significant increase observed with COX inhibition after AA release by IND and CXB suggest that these granules may be storage units for AA.

It is proven by in vitro and in vivo studies that RMICs synthesize HA [**23**,**27**,**28**]. HA may be regulated depending on the water balance of the organism. Moreover, it has been reported that AVP decreased HA levels [**22**] by increasing hyaluronidase activity [**29**-**31**]. The primary cell receptor for HA is CD44 and it is also identified in RMIHs [**28**]. It is known that this receptor plays a role in cell-cell clustering, matrix-cell interaction, cell migration and receptor-specific HA internalization/fractionation. CD44 is a transmembrane glycoprotein and consists of 4 functional domains. The change of these domains leads to change in the structure and thus, changes in HA binding and the interaction of CD44 with the cytoskeleton. In our findings, we determined a significant increase in medullar HA and CD44 levels in all PGE_2 inhibited groups compared to control, suggesting an inverse relation between PGE_2 inhibition and levels of renal medullar HA and CD44.

Cell viability is also related to PGE_2 inhibition. Studies showed that COX-2 inhibition results in apoptosis in cultured RMICs [**15**-**20**]. Aoudjit et al. reported an anti-apoptotic and protective role of COX-2-originated PGE_2 in glomerular epithelial cells, mediated by EP4 [**32**]. Furthermore, Küper et al. found that PGE_2 inactivates pro-apoptotic protein Bad and protects cell viability in renal medullar epithelial cells [**33**]. In parallel with these findings, we also determined a significant increase in RMIC apoptosis in PGE_2 inhibited animals when compared to controls. These results suggest that PGE_2 inhibition results in RMIC apoptosis.

Conclusion

We suggest that the changes in PGE_2 affects lipid droplets in RMICs quantitatively and qualitatively; these granules may be the storage units for AA; functional changes in RMICs via PGE_2 affects HA levels in medullar interstitium and urine volume; and finally, PGE_2 inhibition results in RMIC apoptosis.

Competing interests

The authors declare that they have no competing interests.

Authors' contributions

Authors' contributions	SDD	HS	HE	LAE	IS
Research concept and design	✓	--	--	--	✓
Collection and/or assembly of data	✓	--	--	--	--
Data analysis and interpretation	✓	✓	✓	--	✓
Writing the article	✓	--	--	--	--
Critical revision of the article	✓	--	--	--	--
Final approval of article	✓	--	--	--	--
Statistical analysis	--	--	--	✓	--

Acknowledgements

This work was supported by Scientific Research Project Coordination Unit of Istanbul University; Project Number: 8402. The authors thank Azize Gumusyazici and Ercument Boztas, the technicians of the electron microscopy laboratory in Istanbul University, Cerrahpasa Medical Faculty.

Publication history

EIC: Gaetano Giuseppe Magro, University of Catania, Italy.
Received: 28-Jul-2017 Final Revised: 29-Sep-2017
Accepted: 30-Oct-2017 Published: 19-Nov-2017

References

1. Maric C, Harris PJ and Alcorn D. **Changes in mean arterial pressure predict degranulation of renomedullary interstitial cells**. *Clin Exp Pharmacol Physiol*. 2002; **29**:1055-9. | Article | PubMed
2. Faber JE, Barron KW, Bonham AC, Lappe R, Muirhead EE and Brody MJ. **Regional hemodynamic effects of antihypertensive renomedullary lipids in conscious rats**. *Hypertension*. 1984; **6**:494-502. | Article | PubMed
3. Kirsten M, MadsenSøren Nielsen C and Craig T. ***The Kidney*, eighthed**. WB Saunders, Boston, 2007.
4. Kaissling B and Le Hir M. **Characterization and distribution of interstitial cell types in the renal cortex of rats**. *Kidney Int*. 1994; **45**:709-20. | Pdf | PubMed
5. Hughes AK, Barry WH and Kohan DE. **Identification of a contractile function for renal medullary interstitial cells**. *J Clin Invest*. 1995; **96**:411-6. | Article | PubMed Abstract | PubMed FullText
6. Hughes AK and Kohan DE. **Mechanism of vasopressin-induced contraction of renal medullary interstitial cells**. *Nephron Physiol*. 2006; **103**:p119-24. | Article | PubMed
7. Muirhead EE, Brooks B, Pitcock JA and Stephenson P. **Renomedullary antihypertensive function in accelerated (malignant) hypertension. Observations on renomedullary interstitial cells**. *J Clin Invest*. 1972; **51**:181-90. | Article | PubMed Abstract | PubMed FullText
8. Lewis DJ and Prentice DE. **Ultrastructure of rhesus monkey renomedullary interstitial cells**. *Lab Anim*. 1979; **13**:75-9. | PubMed
9. Pitcock JA, Brown PS, Brooks B, Clapp WL, Brosius WL and Muirhead EE. **Renomedullary deficiency in partial nephrectomy-salt hypertension**. *Hypertension*. 1980; **2**:281-90. | Article | PubMed
10. Muirhead EE. **Case for a renomedullary blood pressure lowering hormone**. *Contrib Nephrol*. 1978; **12**:69-81. | PubMed
11. Muirhead EE, Rightsel WA, Leach BE, Byers LW, Pitcock JA and Brooks B. **Reversal of hypertension by transplants and lipid extracts of cultured renomedullary interstitial cells**. *Lab Invest*. 1977; **36**:162-72. | PubMed
12. Muirhead EE, Byers LW, Desiderio DM, Brooks B and Brosius WM. **Antihypertensive lipids from the kidney: alkyl ether analogs of phosphatidylcholine**. *Fed Proc*. 1981; **40**:2285-90. | PubMed
13. Muirhead EE. **Discovery of the renomedullary system of blood pressure control and its hormones**. *Hypertension*. 1990; **15**:114-6. | Article | PubMed
14. Zusman RM and Keiser HR. **Prostaglandin biosynthesis by rabbit renomedullary interstitial cells in tissue culture. Stimulation by**

angiotensin II, bradykinin, and arginine vasopressin. *J Clin Invest*. 1977; **60**:215-23. | Article | PubMed Abstract | PubMed FullText

15. Badzynska B and Sadowski J. **Opposed effects of prostaglandin E2 on perfusion of rat renal cortex and medulla: interactions with the renin-angiotensin system**. *Exp Physiol*. 2008; **93**:1292-302. | Article | PubMed
16. Harris RC and Breyer MD. **Physiological regulation of cyclooxygenase-2 in the kidney**. *Am J Physiol Renal Physiol*. 2001; **281**:F1-11. | Article | PubMed
17. Rao R, Hao CM and Breyer MD. **Hypertonic Stress Activates Glycogen Synthase Kinase 3_-mediated Apoptosis of Renal Medullary Interstitial Cells, Suppressing an NF_B-driven Cyclooxygenase-2-dependent Survival Pathway**. *The Journal Of Biological Chemistry.* 2004; **279**:3949–3955. | Pdf
18. Hao CM, Komhoff M, Guan Y, Redha R and Breyer MD. **Selective targeting of cyclooxygenase-2 reveals its role in renal medullary interstitial cell survival**. *Am J Physiol*. 1999; **277**:F352-9. | Article | PubMed
19. Harris RC. **Cyclooxygenase-2 in the kidney**. *J Am Soc Nephrol*. 2000; **11**:2387-94. | Article | PubMed
20. Hao CM, Yull F, Blackwell T, Komhoff M, Davis LS and Breyer MD. **Dehydration activates an NF-kappaB-driven, COX2-dependent survival mechanism in renal medullary interstitial cells**. *J Clin Invest*. 2000; **106**:973-82. | Article | PubMed Abstract | PubMed FullText
21. Goransson V, Johnsson C, Nylander O and Hansell P. **Renomedullary and intestinal hyaluronan content during body water excess: a study in rats and gerbils**. *J Physiol*. 2002; **542**:315-22. | Article | PubMed Abstract | PubMed FullText
22. Rugheimer L, Johnsson C, Maric C and Hansell P. **Hormonal regulation of renomedullary hyaluronan**. *Acta Physiol (Oxf)*. 2008; **193**:191-8. | Article | PubMed
23. Goransson V, Hansell P, Moss S, Alcorn D, Johnsson C, Hallgren R and Maric C. **Renomedullary interstitial cells in culture; the osmolality and oxygen tension influence the extracellular amounts of hyaluronan and cellular expression of CD44**. *Matrix Biol*. 2001; **20**:129-36. | Article | PubMed
24. Dwyer TM, Banks SA, Alonso-Galicia M, Cockrell K, Carroll JF, Bigler SA and Hall JE. **Distribution of renal medullary hyaluronan in lean and obese rabbits**. *Kidney Int*. 2000; **58**:721-9. | Article | PubMed
25. Pitcock JA, Brown PS, Byers W, Brooks B and Muirhead EE. **Degranulation of renomedullary interstitial cells during reversal of hypertension**. *Hypertension*. 1981; **3**:II-75-80. | PubMed
26. Hao CM and Breyer MD. **Hypertension and cyclooxygenase-2 inhibitors: target: the renal medulla**. *Hypertension*. 2004; **44**:396-7. | Article | PubMed
27. Hansell P, Maric C, Alcorn D, Goransson V, Johnsson C and Hallgren R. **Renomedullary interstitial cells regulate hyaluronan turnover depending on growth media osmolality suggesting a role in renal water handling**. *Acta Physiol Scand*. 1999; **165**:115-6. | Article | PubMed
28. Goransson V, Hansell P, Moss S, Alcorn D, Johnsson C, Hallgren R and Maric C. **Renomedullary interstitial cells in culture; the osmolality and oxygen tension influence the extracellular amounts of hyaluronan and cellular expression of CD44**. *Matrix Biol*. 2001; **20**:129-36. | Article | PubMed
29. Ginetzinsky AG. **Role of hyaluronidase in the reabsorption of water in renal tubules: the mechanism of action of the antidiuretic hormone**. *Nature*. 1958; **182**:1218-1219.
30. Nikiforovskaia LF, Tischenko NI and Ivanova LN. **The glycosaminoglycanohydrolases of the rat kidney lacking antidiuretic hormone**. *Sechenov Physiol J USSR*. 1987; **73**:978-985.
31. Hardingham T, Heng BC and Gribbon P. **New approaches to the investigation of hyaluronan networks**. *Biochem Soc Trans*. 1999; **27**:124-7. | Article | PubMed
32. Aoudjit L, Potapov A and Takano T. **Prostaglandin E2 promotes cell survival of glomerular epithelial cells via the EP4 receptor**. *Am J Physiol Renal Physiol*. 2006; **290**:F1534-42. | Article | PubMed
33. Kuper C, Bartels H, Beck FX and Neuhofer W. **Cyclooxygenase-2-dependent phosphorylation of the pro-apoptotic protein Bad inhibits tonicity-induced apoptosis in renal medullary cells**. *Kidney Int*. 2011; **80**:938-45. | Article | PubMed

Citation:
Delipinar SD, Sonmez H, Ekmekci H, Erozenci LA and Seckin I. **The effects of different inhibitory pathways of prostaglandin E_2 biosynthesis on renomedullary interstitial cells in rats: a multidisciplinary study**. *J Histol Histopathol*. 2017; **4**:13. http://dx.doi.org/10.7243/2055-091X-4-13